

Coordination Between TSOs and DSOs: Flexibility Domain Identification

Liliia Ageeva¹, Maryam Majidi², David Pozo^{1}*

¹*Center for Energy Science and Technology, Skolkovo Institute of Science and Technology (Skoltech),
Moscow, Russia*

²*Department of Energy Management and Operation of Electrical Networks, University of Kassel,
Kassel, Germany*

**E-mail: d.pozo@skoltech.ru*

Keywords: Active Distribution Network, DistFlow, LinDistFlow, Epsilon-Constraint Method, TSO-DSO

Abstract

The enormous technological potential accumulated over the past two decades would make possible to change the operating principles of power systems entirely. The consequent technological evolution is not only affecting the structure of the electricity markets, but also the interactions between Transmission System Operators (TSOs) and Distribution System Operators (DSOs). New practical solutions are needed to improve the coordination between the grid operators at the national, TSOs, and local level, DSOs. In this paper, we define the flexibility range of coordination between TSOs and DSOs. By doing so, we propose an algorithm based on epsilon-constrained methods by means of mathematical programming and power systems principles. We evaluate and compare different classical optimal power flow formulations (AC-OPF, DISTFLOW, DISTFLOW-SOCP, and LINDISTFLOW) for building the flexible TSO-DSO flexible domain. The presented approaches in this paper are analyzed in an IEEE 33-bus test radial distribution system. We show that for this particular problem, the DISTFLOW-SOCP has the worst accuracy, despite the popularity among the academic community of convex relaxation approaches.

1 Introduction

The current power energy industry is on the inception of, possible, the largest transformation in its history. The enormous technological potential accumulated over the past two decades would make possible to change the operating principles of power systems entirely. The consequent technological evolution is not only affecting the structure of the electricity markets, but also the interactions between transmission system operator (TSOs) and distribution system operator (DSOs). A new generation of distribution networks are evolving to have an active role in the control and management of every participant connected to it so, power is not anymore unidirectional between distribution and transmission grids. New practical solutions are needed to improve the coordination between the grid operators at the national, TSOs, and local level, DSOs in a reliable, secure, and economic fashion. Solving this problem is vital for the future power system since the number of uncertainties in the grid is rising as a result of widespread distributed energy generation resources, mainly renewable.

One of the crucial points of studying active distribution networks (ADNs) is the flexibility that ADNs can provide to the main grid, i.e., at the transmission level. This can unpin capabilities of providing new services to TSOs from DSOs, like ancillary services. The efficient coordination between TSOs and DSOs could bring some advantages such as congestion management, system balancing, power quality control, enhance real-time control and supervision, and grid infrastructure updates shifting among others.

1.1 State-of-the-Art

Literature related to the TSO-DSO interaction is relatively new. The paper [1] proposes a classification scheme, which is called a taxonomy, for the different types of flexibility, in both research and industrial projects, that are used in electric grids. The study in [2] reviews flexibility products and markets designs and implementations to support the power systems operation by considering the renewable generation and distributed energy resources increases. A modeling framework is presented in [3] to approximate the flexibility of an ADN by the regulation of the power flow over the TSO-DSO interface to provide ancillary services. Correspondingly, the effect of time-invariant influencing factors on the flexibility of the ADN is discussed. In [4], the aggregated flexibility of distribution grids without needing to release sensitive grid data is improved using linear optimization. The proposed model is validated using two real radial MV-level distribution grids in Germany. A robust distributed generation investment planning, which considers the uncertainties associated with the intermittent renewable generation and variable electricity demand, is proposed at [5] to minimize the net present value of total costs. [6] validates an integrated communication and optimization framework for performing the coordination of a TSO congestion relief with a DSO objectives. [7] proposes a methodology toward the calculation of the ADNs flexibility based on the feasibility region at the TSO-DSO interface by employing a Monte Carlo sampling approach. The paper in [8] presents a methodology based on the solution of a set of optimization problems that approximate

the flexibility ranges at TSO-DSO margin while considering the technical limits and a maximum cost that the customer is willing to pay. The flexibility for TSO-DSO plus Retailer coordination in Britain is evaluated in [9].

1.2 Paper Approach and Contributions

This paper defines a flexible region as all the possible values of active and reactive power at the interface TSO-DSO, i.e., substation/s, such as a ADN can operate without violating any technical limits within the ADN. Thus, the principal objective of this work is to identify the boundaries of an active-reactive power at the interface TSO-DSO. For doing so, we employ mathematical programming for finding optimal operating points where active and reactive power at the TSO-DSO interface are cross-examined to their extreme values while keeping feasible the distribution grid operation. We propose an epsilon-constrained optimization method that, contrary to Monte-Carlo-based methods, does not require a large number of simulations. Besides, we argue that Monte-Carlo-based methods are not appropriate for feasible domain construction. The feasible domain should be built on the basis of the (single) optimal operating dispatch point by finding the largest capacity that flexible resources and distribution grid can provide by “stressing” them but not formed by different loading conditions that imply different dispatch.

The main contributions of this work are in two main directions.

- *On the methodology.* We propose a methodology based on the epsilon-constraint method, adopted from multi-objective optimization, to construct the boundaries of the TSO-DSO feasible regions that efficiently generate the feasible region with a very small number of simulations. Opposite to Monte Carlo methods, the number of simulations needed for feasible region construction does not depend on the control and uncertain parameters of the ADNs;
- *On the analysis* The above contribution is supported by an optimal power flow (OPF). There are several OPF models the literature. We identified four of the most common OPF approaches for the optimal operation of ADNs, so called, (i) alternating current optimal power flow, AC-OPF, (ii) an ad-hoc reformulation for the AC-OPF for distribution grids, DISTFLOW, (iii) a convexified version of the DISTFLOW model based on second-order cone programming, DISTFLOW-SOCP, and (iv) a linearized version of DISTFLOW, LINDISTFLOW. The epsilon-constrained method is tested in the IEEE 33-bus distribution network and compared for each OPF model.

1.3 Paper Organization

This paper is structured as follows. In Section 2, different OPF methods in distribution grids are presented for a single-period case. Section 3 presents the epsilon constraint method as the main methodology to define TSO-DSO feasibility region. Section 4 presents the case study. Finally, conclusion is given in Section 5.

2 Optimal Power Flow in Distribution Grids

The purpose of utilizing the OPF is determining the optimal operating point for an electric power system relative to desired objectives, such as minimizing generation cost and losses. Along with that, the solution must fulfill the constraints that model the power flow physics and enforce technical limits [10]. The general form of the cost-prioritized OPF objective function is defined in (1). The first term represents the cost/benefits from the power requested/injected from/to the main grid. The second term represents the generation cost within the DSO.

$$\min \left(c^{se} p^{se} + \sum_{i \in \mathcal{N} \setminus \{1\}} c_i p_i^G \right) \quad (1)$$

The cost term at the TSO-DSO interface, c^{se} , is assumed to be symmetric in here. Thus, power withdraw from the substation has the same cost that the payment received for the power injected to the substation. The term p^{se} takes positive value when power flows from TSO to DSO and negative when it flows from DSO to TSO. As customary in literature, we have assigned the bus number one to the substation. Also, we have modeled a single substation without loss of generality. Various versions of the OPF problem are introduced in the next subsections.

2.1 AC-OPF Formulation

The AC-OPF is the most common representation of the full AC power flow equations and operational limits associated with the power grid. It is based on the nodal power flows in a electric network. The AC-OPF is a non-linear and non-convex optimization problem. Thus, no global optimum solution is guaranteed for this problem [11].

The nodal balance equations for the active and reactive power are formulated in (2) and (3), respectively.

$$p_i^G - p_i^D - \sum_{j: (i,j) \in \mathcal{L}} p_{ij} = 0, \quad \forall i \in \mathcal{N} \quad (2)$$

$$q_i^G - q_i^D + q_i^C - \sum_{j: (i,j) \in \mathcal{L}} q_{ij} = 0, \quad \forall i \in \mathcal{N} \quad (3)$$

We have assumed a single generator and single load/demand at each node i , for the sake of simplicity.

The branch active and reactive power flow, p_{ij}/q_{ij} , are given by equations (4) and (5), respectively.

$$p_{ij} = v_i^2 Y_{Lij} \cos(\theta_{Lij}) - v_i v_j Y_{Lij} \cos(\delta_i - \delta_j - \theta_{Lij}) + \frac{1}{2} v_i^2 Y_{Sij} \cos(\theta_{Sij}), \quad \forall (i, j) \in \mathcal{L} \quad (4)$$

$$q_{ij} = -v_i^2 Y_{Lij} \sin(\theta_{Lij}) - v_i v_j Y_{Lij} \sin(\delta_i - \delta_j - \theta_{Lij}) - \frac{1}{2} v_i^2 Y_{Sij} \sin(\theta_{Sij}), \quad \forall (i, j) \in \mathcal{L} \quad (5)$$

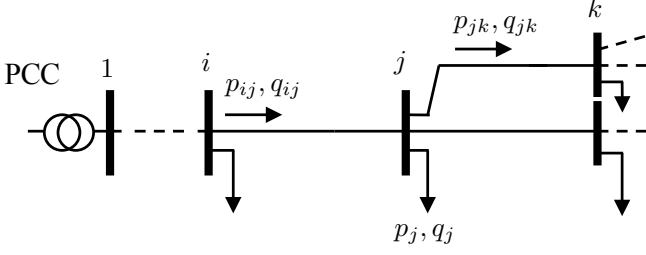


Fig. 1: Power flow notations in a radial network

The active and reactive power lower and upper bound of each generation units are defined as:

$$p_i^{G,\min} \leq p_i \leq p_i^{G,\max}, \quad \forall i \in \mathcal{N} \quad (6)$$

$$q_i^{G,\min} \leq q_i \leq q_i^{G,\max}, \quad \forall i \in \mathcal{N} \quad (7)$$

The line capacity, nodal voltage limits, and capacitor banks constraints are formulated in (8), (9) and (10), respectively:

$$p_{ij}^2 + q_{ij}^2 \leq (s_{ij}^{\max})^2, \quad \forall (i, j) \in \mathcal{L} \quad (8)$$

$$v_i^{\min} \leq v_i \leq v_i^{\max}, \quad \forall i \in \mathcal{N} \quad (9)$$

$$0 \leq q_i^C \leq q_i^{C,\max}, \quad \forall i \in \mathcal{N} \quad (10)$$

Finally, the boundary conditions at the substation are given by:

$$v_1 = 1, \quad (11)$$

$$p^{\text{se}} = p_1^G, \quad q^{\text{se}} = q_1^G \quad (12)$$

2.2 DISTFLOW Formulation

The OPF for distribution network could be represented by the single-phase recursive branch-flow equations based on the Kirchhoff's and the Ohm's law at every bus; known as DISTFLOW equations. This formulation is introduced in the seminal works of *Baran and Wu* [12], [13]. Fig. 1 provides notation used in here for power flow equation in radial distribution networks. Thus, the DISTFLOW equations are formulated as:

$$p_{ij} = p_j + r_{ij}l_{ij} + \sum_{k:(j,k) \in \mathcal{L}} p_{jk}, \quad \forall (i, j) \in \mathcal{L} \quad (13)$$

$$q_{ij} = q_j + x_{ij}l_{ij} + \sum_{k:(j,k) \in \mathcal{L}} q_{jk}, \quad \forall (i, j) \in \mathcal{L} \quad (14)$$

$$v_j^2 = v_i^2 + (r_{ij}^2 + x_{ij}^2)l_{ij} - 2(r_{ij}p_{ij} + x_{ij}q_{ij}), \quad \forall (i, j) \in \mathcal{L} \quad (15)$$

$$p_{ij}^2 + q_{ij}^2 = l_{ij}v_i^2, \quad \forall (i, j) \in \mathcal{L} \quad (16)$$

where p_{ij} and q_{ij} are active and reactive branch power flow from node i to j . l_{ij} , r_{ij} and x_{ij} are the current squared, resistance, and reactance of the branch ij , respectively. p_j and q_j are the net active and reactive power withdraw at node j ,

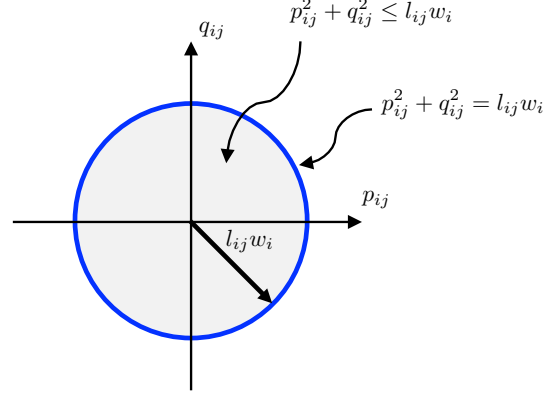


Fig. 2: Equation (16) and its relaxation (20) projected onto p_{ij} - q_{ij} orthant

represented by (17) and (18), respectively.

$$p_j = p_j^D - p_j^G, \quad \forall j \in \mathcal{N} \quad (17)$$

$$q_j = q_j^D - q_j^C - q_j^G, \quad \forall j \in \mathcal{N} \quad (18)$$

Note that power flow equations (2)–(5) from AC-OPF formulation are replaced by the equations (13)–(18) in the DISTFLOW formulation. The later, has linear definition for the branch flows, (13) and (14), while the AC-OPF are non-linear. Yet, (14) and (15) are non-linear and non-convex. The technical constraints concerning voltage, generation, and line limits are the same for the DISTFLOW.

2.3 DISTFLOW-SOCP Formulation

In this subsection we transform the non-convex DISTFLOW formulation into a convex one. First, we replace $v_i^2 = w_i$. Thus, the non-linear equation (15) is exactly reformulated as a linear one, (19).

$$w_j = w_i + (r_{ij}^2 + x_{ij}^2)l_{ij} - 2(r_{ij}p_{ij} + x_{ij}q_{ij}), \quad \forall (i, j) \in \mathcal{L} \quad (19)$$

Next, we can relax the the non-convex equality (16) by a convex inequality constraint as follows (see Fig. 2 for graphical interpretation):

$$p_{ij}^2 + q_{ij}^2 \leq l_{ij}w_i, \quad \forall (i, j) \in \mathcal{L} \quad (20)$$

where term $l_{ij}w_i$ is still a bilinear term, but it can be reformulated as $l_{ij}w_i = \left(\frac{l_{ij}+w_i}{2}\right)^2 - \left(\frac{l_{ij}-w_i}{2}\right)^2$. Therefore, equation (20) can be recast as the convex conic constraint (21).

$$p_{ij}^2 + q_{ij}^2 + \left(\frac{l_{ij}-w_i}{2}\right)^2 \leq \left(\frac{l_{ij}+w_i}{2}\right)^2, \quad \forall (i, j) \in \mathcal{L} \quad (21)$$

The resulting OPF problem is convex; in particular, this problem is classified as a second-order cone programming (SOCP). We refer to this OPF formulation as DISTFLOW-SOCP. Existing methods for solving this class of problems guarantee global solutions [14].

Table 1 Summary for the single-period OPF models used for feasible region construction

Set of constraints/objective	AC-OPF	DISTFLOW	DISTFLOW-SOCP	LINDISTFLOW
Objective	(1)	(1)	(1)	(1)
Power Flow Constraints	(2)–(5)	(13)–(18)	(13), (14), (19), (22), (17), (18)	(24)–(26), (17), (18)
Technical limits	(6)–(10)	(6)–(10)	(6)–(8), (10), (22)	(6)–(7), (10), (22), (27)
Boundary conditions at SE	(11), (12)	(11), (12)	(12), (23)	(12), (23)
	AC-OPF	DISTFLOW	DISTFLOW-SOCP	LINDISTFLOW
Type of power flow approach	true representation	true representation	relaxation	approximation
Optimization class	NLP	NLP	SOCP	LP

As in the DISTFLOW formulation, technical constraints for the system operation are the same as in the AC-OPF formulation. However, in this case, we need to reformulate constraints related to the voltage magnitude. Therefore, voltage limits (9) are replaced by (22). Likewise, boundary condition (11) at substation is substituted by (23).

$$(v_i^{\min})^2 \leq w_i \leq (v_i^{\max})^2, \quad \forall i \in \mathcal{N} \quad (22)$$

$$w_1 = 1 \quad (23)$$

2.4 LINDISTFLOW Formulation

Baran and Wu [12] introduced a linearized version of the DISTFLOW, the LINDISTFLOW model. Later, Low reviewed it in [15]. LINDISTFLOW assumes no losses. The LINDISTFLOW is reformulated from the extract OPF formulation for radial networks (DISTFLOW formulation), resulting in a linear approximation, attractive for engineers and economists many reasons. The LINDISTFLOW power flow equations are stated as follow:

$$p_{ij} = p_j + \sum_{k:(j,k) \in \mathcal{L}} p_{jk}, \quad \forall (i,j) \in \mathcal{L} \quad (24)$$

$$q_{ij} = q_j + \sum_{k:(j,k) \in \mathcal{L}} q_{jk}, \quad \forall (i,j) \in \mathcal{L} \quad (25)$$

$$w_i - w_j = 2(r_{ij}p_{ij} + x_{ij}q_{ij}), \quad \forall (i,j) \in \mathcal{L}. \quad (26)$$

The technical constraints and boundary conditions are set like in the AC-OPF formulation, except for line limits constraints (8), that is substituted by (27) in order to linearize have a full linear model.

$$p_{ij} \leq p_{ij}^{\max}, q_{ij} \leq q_{ij}^{\max}, \quad \forall (i,j) \in \mathcal{L} \quad (27)$$

2.5 OPF Formulation Summary

In Table 1 we have summarized the set of constraints and objective function for each of the fourth formulations that we would like to analyze for flexibility region construction. The main differences among formulations are in the power flow representation. While AC-OPF and DISTFLOW contains exact representation of the power flows equations, DISTFLOW-SOCP is relaxation, and LINDISTFLOW is an approximation of the true power flow equations.

3 Epsilon-Constraint Method

To define a feasible region between TSO-DSO, many scenario-based methods, such as Monte Carlo [7], are introduced in the literature. Scenario-based Monte Carlo simulation provides various operating points as scenarios; the model is a cloud of the operating points, and also the finite number of scenarios treats properly for convex problems. However, it requires an extensive data set, as the large vectors of uncertainty increase the number of scenarios required to construct the region. In this paper, we find the operational limits of the ADN, which implicitly depends on the optimal operating dispatch. For doing so, we solve the multi-objective optimization problem for finding the maximum and minimum of active and reactive power at the PCC (28), while satisfying grid feasibility (i.e., power flow constraints, technical limits and boundary conditions – see Table 1 rows 2–4) for given optimal injections. Grid feasibility is represented by \mathcal{F} in the multi-objective problem (28).

$$\begin{aligned} \max / \min \quad & \{p^{se}, q^{se}\} \\ \text{s.t:} \quad & (p^{se}, q^{se}) \in \mathcal{F}(p_i^*, q_i^*, i \in \mathcal{N} \setminus \{1\}) \end{aligned} \quad (28)$$

The solution of (28) is a Pareto front (the feasible region in our case) rather than a single operational point. One of the most well-known methods to solve (28) is the so-called epsilon-constraint method [16]. In this method a primary objective function is considered while the other objective functions are relaxed with the set of constraints. Perturbations on ϵ_i size are added to the objectives in the set of constraints and solved sequentially.

Thus, the TSO-DSO feasible region can be reconstructed by solving a sequential set of problems. For the particular iteration κ , the problem to solve is depicted in (29), where $q^{se(\kappa)}$ is updated in each iteration. Figure 3 represents the schematic feasibility region created by the epsilon-constraint method.

$$\begin{aligned} \max / \min \quad & p^{se} \\ \text{s.t:} \quad & (p^{se}, q^{se}) \in \mathcal{F}(p_i^*, q_i^*, i \in \mathcal{N} \setminus \{1\}) \\ & q^{se(\kappa)} - \frac{\epsilon}{2} \leq q^{se} \leq q^{se(\kappa)} + \frac{\epsilon}{2} \end{aligned} \quad (29)$$

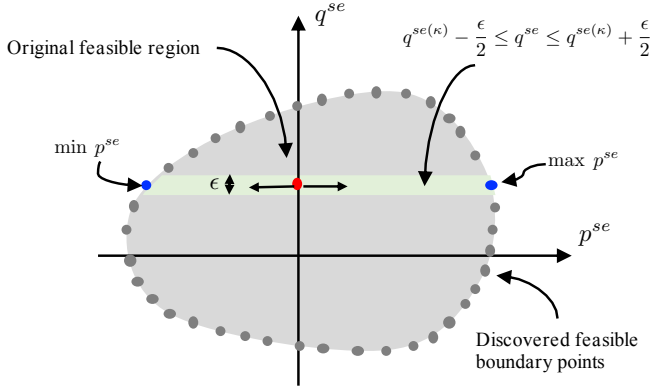


Fig. 3: Concept of the feasibility region construction by epsilon-constraint method

The stopping criterion is set for a given number N of points that will form the boundary accordingly to the resolution needed. Then, the value of ϵ can be computed to equally divide the continuous space of feasible values of q^{se} [16].

4 Case Study

We have used the IEEE 33-bus radial distribution system for testing our method. We have modified this case by including four fast distributed generators (DGs) in Fig. 4. Capacitor banks of 1MVar are connected to nodes 10, 20 and 30. Node 1 is the slack node and the defines as the PCC, where is the interface between transmission and distribution network. Twenty-four hours were simulated. We chose 200 points for building feasible boundaries for all case studies.

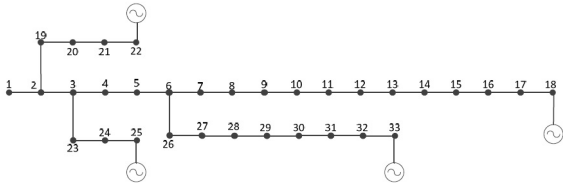


Fig. 4: 33-bus radial distribution system

The implementation of the OPF models was done using Julia 1.4, and JuMP 0.19, with the solvers Ipopt 0.5.4 for NLP problems and Gurobi 9.0. for SOCP and LP problems. All simulations were performed in a Laptop Intel(R) Core(TM) i5-6200U CPU with installed RAM 8GB. Note that for solving the sequence of NLP in the AC-OPF and DISTFLOW, we have provided starting point to Ipopt based on previous iteration.

Table 2 summarizes the computation time for each model. We observe the efficiency of DISTFLOW with respect to the AC-OPF formulation with a time reduction of about 1/3. The LINDISTFLOW method, of course, is the fastest one, about $780\times$ faster than AC-OPF, and $290\times$ faster than DISTFLOW.

Figure 5 represents the reconstruction for the feasible domain for the hour 14 at the interface TSO-DSO. Both

Table 2 CPU time for building feasible regions with epsilon constraint method

Model	CPU time [seconds]
AC-OPF	1798.3
DISTFLOW	666.2
DISTFLOW-SOCP	478.8
LINDISTFLOW	2.3

AC-OPF and DISTFLOW are the same and depicted in red. The black circles denote the LINDISTFLOW, and green squares represent the feasible domain when using a relaxed formulation DISTFLOW-SOCP. The relaxed formulation overestimates the active power that the ADN can absorb (positive orthant). At the same time, the DISTFLOW-SOCP quite well approximates the power available to inject into the transmission grid. On the other hand, the LINDISTFLOW is approaching very close to the exact feasible domain. But, it has the main discrepancies in the negative orthant, i.e., active power that could be injected from the ADN to the transmission grid. This is mainly because the LINDISTFLOW does not consider losses overestimating the capability of energy that could be generated from the ADN.

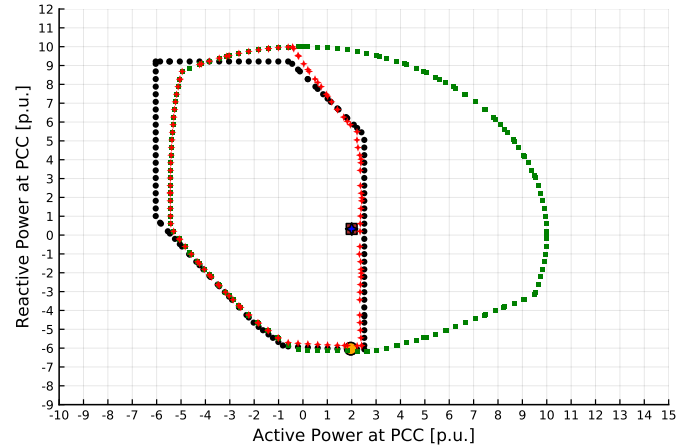


Fig. 5: Feasibility region constructed with the epsilon constraint method for period 14. Black circles for LINDISTFLOW model, red stars for DISTFLOW and AC-OPF model, and green squares for DISTFLOW-SOCP model.

Fig. 6 shows four consecutive hours resulting from the feasible region generation. It is worth noting that even we have omitted in our formulation the multi-period OPF, it has implemented in a multi-period fashion, and it can be easily extended and include inter-temporal constraints related to energy storage or ramping capabilities.

5 Conclusions and Discussion

In this paper, we have defined the flexibility region of an ADN (DSO level) connected to a TSO based on mathematical programming and power systems principles. This work evaluates and compares different optimal power flow formulations (AC-OPF, DISTFLOW, DISTFLOW-SOCP, and

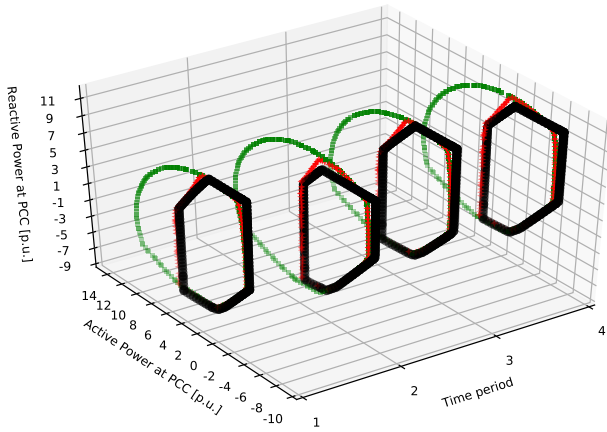


Fig. 6: Feasibility region for four consecutive periods

LINDISTFLOW), commonly used in the literature, for building feasible regions for TSO-DSO interaction. An epsilon-constraint method is proposed for constructing the feasible operation region at the TSO-DSO interface.

The presented method is analyzed in an IEEE 33-bus test radial distribution system. The solutions obtained are compared for each model and proposed. We have observed that LINDISTFLOW is fast and relatively closed to the exact original feasible region. On the other hand, the convex relaxation DISTFLOW-SOCP showed large discrepancies with regard to the exact feasible limits. This raises an attention note on the use of convexification models. Finally, results from this research work could help to contribute in future and open challenges for an advanced TSO-DSO cooperation.

6 Acknowledgements

This work was supported by Skoltech NGP Program (Skoltech-MIT joint project)

References

- [1] R. Bärenfänger, E. Drayer, D. Daniluk, B. Otto, E. Vanet, R. Caire, T. S. Abbas, and B. Lisanti, “Classifying flexibility types in smart electric distribution grids: a taxonomy,” in *CIREN Workshop 2016*. IET, 2016, pp. 1–4.
- [2] J. Villar, R. Bessa, and M. Matos, “Flexibility products and markets: Literature review,” *Electric Power Systems Research*, vol. 154, pp. 329–340, 2018.
- [3] D. M. Gonzalez, J. Hachenberger, J. Hinker, F. Rewald, U. Häger, C. Rehtanz, and J. Myrzik, “Determination of the time-dependent flexibility of active distribution networks to control their tso-dso interconnection power flow,” in *2018 Power Systems Computation Conference (PSCC)*. IEEE, 2018, pp. 1–8.
- [4] D. A. Contreras and K. Rudion, “Improved assessment of the flexibility range of distribution grids using linear optimization,” in *2018 Power Systems Computation Conference (PSCC)*. IEEE, 2018, pp. 1–7.
- [5] T. Ji, J. Yao, Y. Wu, A. Ehsan, M. Cheng, and Q. Yang, “Robust active distribution network planning considering stochastic renewable distributed generation,” in *2018 37th Chinese Control Conference (CCC)*. IEEE, 2018, pp. 8803–8808.
- [6] R. T. Elliott, R. Fernandez-Blanco, K. Kozdras, J. Kaplan, B. Lockyear, J. Zyskowski, and D. S. Kirschen, “Sharing energy storage between transmission and distribution,” *IEEE Transactions on Power Systems*, vol. 34, no. 1, pp. 152–162, 2018.
- [7] L. Ageeva, M. Majidi, and D. Pozo, “Analysis of feasibility region of active distribution networks,” in *2019 International Youth Conference on Radio Electronics, Electrical and Power Engineering (REEPE)*. IEEE, 2019, pp. 1–5.
- [8] J. Silva, J. Sumaili, R. J. Bessa, L. Seca, M. A. Matos, V. Miranda, M. Caujolle, B. Goncer, and M. Sebastian-Viana, “Estimating the active and reactive power flexibility area at the tso-dso interface,” *IEEE Transactions on Power Systems*, vol. 33, no. 5, pp. 4741–4750, 2018.
- [9] A. V. Pastor, J. N. Martin, D. W. Bunn, and A. Laur, “Evaluation of flexibility markets for retailer-dso-tso coordination,” *IEEE Transactions on Power Systems*, 2018.
- [10] A. J. Wood, B. F. Wollenberg, and G. B. Sheblé, *Power generation, operation, and control*. John Wiley & Sons, 2013.
- [11] D. K. Molzahn, I. A. Hiskens *et al.*, “A survey of relaxations and approximations of the power flow equations,” *Foundations and Trends® in Electric Energy Systems*, vol. 4, no. 1-2, pp. 1–221, 2019.
- [12] M. Baran and F. F. Wu, “Optimal sizing of capacitors placed on a radial distribution system,” *IEEE Transactions on power Delivery*, vol. 4, no. 1, pp. 735–743, 1989.
- [13] M. E. Baran and F. F. Wu, “Optimal capacitor placement on radial distribution systems,” *IEEE Transactions on power Delivery*, vol. 4, no. 1, pp. 725–734, 1989.
- [14] F. Alizadeh and D. Goldfarb, “Second-order cone programming,” *Mathematical programming*, vol. 95, no. 1, pp. 3–51, 2003.
- [15] S. H. Low, “Convex relaxation of optimal power flow—part I: Formulations and equivalence,” *IEEE Transactions on Control of Network Systems*, vol. 1, no. 1, pp. 15–27, 2014.
- [16] Y. Haimes, L. S. Lasdon, and D. Wismer, “On a bicriterion formation of the problems of integrated system identification and system optimization,” *IEEE Transactions on Systems, Man and Cybernetics*, no. 3, pp. 296–297, 1971.